*Available online www.jocpr.com*

**Journal of Chemical and Pharmaceutical Research, 2015, 7(8):44-53**

**Research Article**

**ISSN : 0975-7384**
**CODEN(USA) : JCPRC5**

# Corrosion inhibition of mild steel in 1 M HCl Solution by hydroxyapatite

**L. Chafki[1], M. Galai[2], E. H. Rifi[1], R. Touir[2*], M. Ebn Touhami[2], Z. Hatim[3] and A. Tazouti[2]**

[1]*Laboratoire de synthèse organique et procédés d'extraction, Université Ibn Tofaïl, Faculté des Sciences, Kenitra, Morocco*
[2]*Laboratoire des Matériaux, d'Electrochimie et d'Environnement, Université Ibn Tofail, Faculté des Sciences, Kénitra, Morocco*
[3]*Laboratoire d'Electrochimie et Traitement de Surface, Université chouaib doukkali, Faculté des sciences, El Jadida, Morocco*

---

**ABSTRACT**

*The inhibition corrosion of mild steel in 1 M HCl medium by hydroxyapatite (HAP) was investigated using potentiodynamic polarization curve and electrochemical impedance spectroscopy. The obtained results showed that the HAP has good corrosion inhibition properties for mild steel in acidic medium and its inhibition increase with concentration and reaches a maximum of 90 % at $10^{-3}$ M. in addition, the impedance diagrams showed one capacitive loop attributed to the charge transfer process on a heterogeneous surface for all concentrations of HAP. However, the adsorption of this apatite at the metallic surface is a physisorption type and follows the Langmuir isotherm adsorption. In the other, the HAP takes its performance at the temperature range 298 K- 328 K and increases with immersion time.*

**Keywords**: Hydroxyapatite; Corrosion inhibition; hydrochloride acid; Mild steel; Electrochemical measurements.

---

## INTRODUCTION

The consequences of corrosion metals and alloys are important in the energy production areas **[1]**, engineering **[2]**, transport, machinery, medical materials **[3]**, microelectronic components, etc. Corrosion is not only wasteful of raw materials and energy, it can cause more accidents with serious consequences and in some cases, contribute to pollution of the environment **[4]**.

However, due to the viability of the steel, the high cost of production and installations, most industries have adopted several measures to prolong the life of this precious metal **[5]**. In recent years, due to the interest in the environment protection and the harmful effects of the use of chemicals on the ecological balance, the traditional approach of corrosion inhibitors has gradually changed **[6]**. Studies, therefore, focus on non-toxic corrosion inhibitors **[7-12]**. For this the inorganic inhibitors which their actions are generally the result of their adsorption on metallic surface are the most commonly used. So, hydroxyapatite has received considerable attention due to its industrial interests, technology and biotechnology. It is used as a catalyst in various reactions such as dehydration and decomposition of alcohols **[13]**, the oxidation of methane **[14-16]** and the conversion of benzene to phenol **[17]**. In addition, it is used as adsorbents for the separation of proteins [18, 19] and as an ion exchange for many metal cations **[20, 21]**.

In this work, the inhibition efficiency of HAP for mild steel in 1 M HCl was studied using electrochemical measurements. The effect of temperature and immersion time was studied.

## EXPERIMENTAL SECTION

### 2.1. Material and compound:

The inhibitor used in this work is the phosphate hydroxyapatite ($Ca_{10}(PO_4)_6OH_2$) and its chemical structure is shown in Figure 1. The hydroxyapatite, a natural form of calcium apatite with the formula $Ca_5(PO_4)_3(OH)$ is often presented in the formulation $Ca_{10}(PO_4)_6(OH)_2$ highlighting the presence of two groups per unit cell (Figure 1).

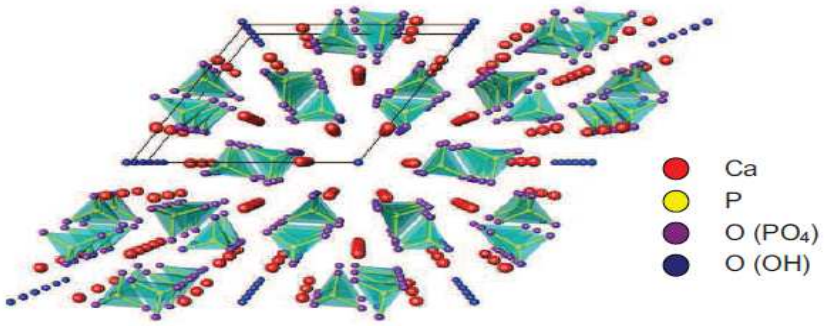


**Figure 1: Structure of the hydroxyapatite mesh, projection along the axis (001) [22]**

The metal used in this study is mild steel which its chemical composition is presented in Table 1. The aggressive solution (1 M HCl) was prepared by dilution of HCl for quality analysis to 37 % with distilled water.

**Table 1: Chemical composition of low carbon steel used (in wt. %)**

| C | Si | Mn | Cr | Mo | Ni | Al | Cu | Co | V | W | Fe |
|---|---|---|---|---|---|---|---|---|---|---|---|
| 0.11 | 0.24 | 0.47 | 0.12 | 0.02 | 0.1 | 0.03 | 0.14 | <0.0012 | <0.003 | 0.06 | Balance |

**2.3. Electrochemical measurements**

Electrochemical measurements were carried out using potentiostat / galvanostat / PGZ100. A classical three electrodes system was used for these studies. Mild steel specimens, platinum (Pt) and Ag/AgCl were used as a working, auxillary and reference electrodes, respectively. All electrochemical experiments were conducted at 298 ± 2 K using 50 mL of test solution with 30 min of immersion time.

The Tafel polarization curves were recorded by scanning the electrode potential from - 900 mV to -100 mV/Ag/AgCl with a scanning rate of 1 mV/s. To evaluate corrosion kinetic parameters, a fitting by Stern-Geary equation was used. To do so, the overall current density values, *i*, were considered as the sum of two contributions, anodic and cathodic current $i_a$ and $i_c$, respectively. For the potential domain not too far from the open circuit potential, it may be considered that both processes followed the Tafel law [**23**]. Thus, it can be derived from equation (1):

$$i = i_a + i_c = i_{corr}\left\{\exp\left[b_a \times (E - E_{corr})\right] - \exp\left[b_c \times (E - E_{corr})\right]\right\} \quad (1)$$

where $i_{corr}$ is the corrosion current density (A cm$^{-2}$), $b_a$ and $b_c$ are the Tafel constants of anodic and cathodic reactions (V$^{-1}$), respectively. These constants are linked to the Tafel slopes $\beta$ (V/dec) in usual logarithmic scale given by equation (2):

$$\beta = \frac{\ln 10}{b} = \frac{2.303}{b} \quad (2)$$

The corrosion parameters were then evaluated by means of nonlinear least square method by applying equation (2) using Origin software. However, for this calculation, the potential range applied was limited to ±0.100V around $E_{corr}$, else a significant systematic divergence was sometimes observed for both anodic and cathodic branches.

The corrosion inhibition efficiency is evaluated from the corrosion current densities values using the relationship (3):

$$\eta_{PP} = \frac{i^0_{corr} - i_{corr}}{i^0_{corr}} \times 100 \quad (3)$$

where $i^0_{corr}$ and $i_{corr}$ are the corrosion current densities values without and with inhibitor, respectively.

The electrochemical impedance spectroscopy measurements were carried out using a transfer function analyzer (VoltaLab PGZ 100), with a small amplitude a.c. signal (10 mV rms), over a frequency domain from 100 kHz to 100 mHz with five points per decade. The EIS diagrams were done in the Nyquist representation. The results were then analyzed in terms of an equivalent electrical circuit using Bouckamp program [**24**].

The inhibiting efficiency derived from EIS, $\eta_{EIS}$ is also added in Table 4 and calculated using the following equation (4):

$$\eta_{EIS} = \frac{R_{ct} - R_{ct}^{0}}{R_{ct}} \times 100 \quad (4)$$

where $R_{ct}^{0}$ and $R_{ct}$ are the charge transfer resistance values in the absence and in the presence of inhibitor, respectively.

## RESULTS AND DISCUSSION

### 3.1. Potentiodynamic polarization curves

The potentiodynamic polarization curves obtained from the corrosion behavior of mild steel in 1 M HCl in the absence and presence of HAP are shown in Figure 2. Their corresponding electrochemical parameters are listed in Table 2. It is seen that the addition of HAP acted on the anodic branches and shifted the corrosion potential to anodic direction. Therefore, it is could be classified as the anodic type corrosion inhibitor. In addition, the reduction of $i_{corr}$ is pronounced more and more with increasing inhibitor concentration. The increased inhibition efficiency with inhibitor concentration indicates that the tested compound acts by adsorption on the metallic surface **[25]**.

However, Table 2 showed that the inhibitor addition may shift the equilibrium corrosion process to the passive direction causing a formation of thin passivation oxide film over the anodic sites, which may increase the anodic potential and depressed the oxidation process. Thus, this reveals that all inhibitors act as mixed type inhibitor with predominant anodic effectiveness. It is noted also that the inhibition was more pronounced with the increase of inhibitor concentration to reach a maximum of 91 % at $10^{-3}$ M of HAP.

In the However, the cathodic Tafel slopes ($\beta_c$) remain constant indicating that the HAP does not change the hydrogen evolution mechanism. Thus, the reduction of $H^+$ ions at the mild steel surface takes place mainly through a charge transfer mechanism [**26, 27**]. Therefore the inhibition effect of the inhibitor may be caused by the simple blocking effect, namely the reduction of reaction area sites on the corroding surface [**28, 29**].

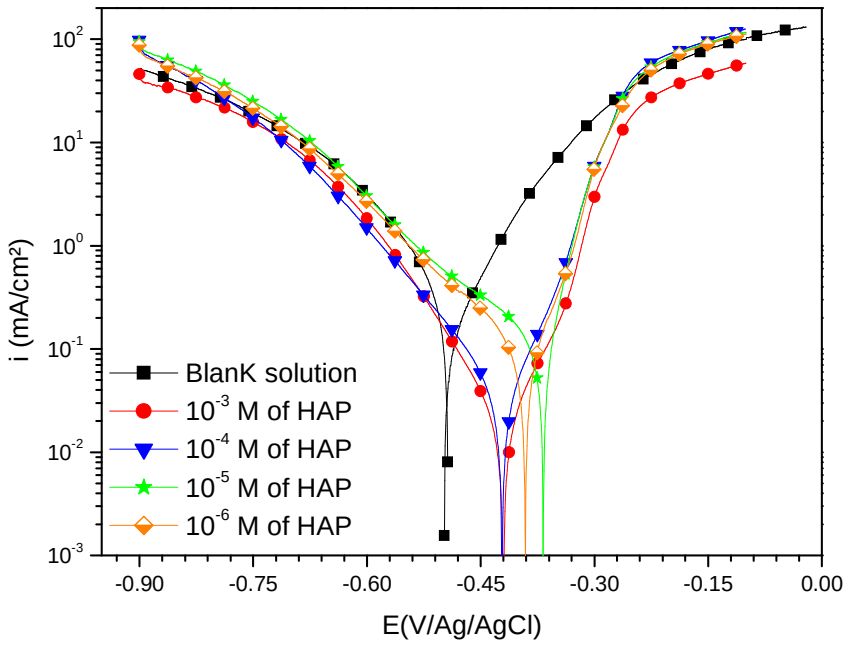


**Figure 2: Potentiodynamic polarization curves of mild steel in 1 M HCl at different concentration of HAP**

On the other hand, the anodic and cathodic Tafel slops remain also constant with HAP addition. This can be explained that the metal dissolution reaction doesn't depend on the applied potential, as it can be seen from the anodic part of Figure 2. Although the iron dissolution rate reduces gradually with the presence of inhibitor at low

anodic over-potentials below – 300 mV/SCE and increases sharply when the applied potential is screened to more anodic values. This potential is generally defined as the desorption potential [**30**]. Therefore, it is concluded that, the adsorption of the inhibitor molecules on metallic surface yields a film formation, which provides a good protection for the mild steel at low anodic over-potentials. However, this film loses its performance at high anodic potential regions. The observed behavior could be explained by the significant iron dissolution, leading to desorption of the formed film from the metal surface.

**Table 2: Electrochemical parameters of mild steel in 1 M HCl in the presence of different concentration of HAP**

| Conc. (M) | $E_{corr}$ (mV/Ag/AgCl) | $i_{corr}$ (µ Acm$^{-2}$) | $\beta_a$(mV dec$^{-1}$) | $\beta_c$(mV dec$^{-1}$) | $\eta_{PP}$(%) |
|---|---|---|---|---|---|
| 00 | -498 | 467 | 70 | 153 | - |
| $10^{-6}$ | -391 | 140 | 54 | 146 | 70 |
| $10^{-5}$ | -362 | 130 | 43 | 147 | 72 |
| $10^{-4}$ | -418 | 46 | 59 | 92 | 90 |
| $10^{-3}$ | -419 | 43 | 66 | 77 | 91 |

### 3.2. Electrochemical impedance spectroscopy:

The representative Nyquist plots of mild steel electrode in 1 M HCl solution in the absence and presence of various concentrations of HAP at corrosion potential is shown in Figure 3. It is noted that all plots contain a slightly depressed semi-circular shape and only one time constant was appeared indicating that the mild steel corrosion is mainly controlled by a charge transfer process. In this case, the equivalent electric circuit, Figure 4, with one time constants was proposed to reproduce these results by non linear regression calculation.

It is worth pointing out that the application of an electrical circuit consisting of double layer capacitor does not always enable achieving satisfactory fitting to the experimental impedance data. The dispersion of the impedance data can be attributed to the surface heterogeneity resulting from the inhibitor's adsorption (mainly), surface roughness, dislocations, impurities, grain boundaries, fractality, etc. In such case using an equivalent electrical circuit employing the double layer capacitance element is not a good enough approximation. The Constant Phase Element (*CPE*) was suggested instead of $C_{ct}$. So, the more heterogeneous surface, hence the higher $n$ values, the greater deviation from ideal capacitative behavior. It allows employing *CPE* element in order to investigate the inhibitive film properties on metallic surface. Thus, the impedance of the *CPE* can be described by the following equation:

$$Z_{\mathrm{CPE}} = \left[ Q\,(j\,\omega)^{n} \right]^{-1} \tag{5}$$

where $j$ is the imaginary number, $Q$ is the frequency independent real constant, $\omega = 2\pi f$ is the angular frequency (rad s$^{-1}$), $f$ is the frequency of the applied signal, $n$ is the *CPE* exponent for whole number of $n$ = 1, 0, -1, *CPE* is reduced to the classical lump element-capacitor ($C$), resistance ($R$) and inductance ($L$) [**31**]. The use of these parameters, similar to the constant phase element (*CPE*), allowed the depressed feature of Nyquist plot to be reproduced readily. However, the effective calculated double layer capacitance ($C$) derived from the *CPE* parameters according to the following equation [**32**]:

$$C = Q^{\frac{1}{\alpha}} \times R^{\frac{(1-\alpha)}{\alpha}} \tag{6}$$

The most important data obtained from the equivalent circuit are presented in Table 3. It may be remarked that $R_{ct}$ value increases and $C_{ct}$ decreases with inhibitor concentration indicating that more inhibitor molecules are adsorbed on metallic surface and provided better surface coverage and/or enhanced the thickness of the protective layer at the metal/solution interface [**33, 34**].

In addition, it is shown that the $n$ values increase from 0.8 to 0.9 with inhibitor concentration, which could be related to the decrease of the surface heterogeneity as a result of the HAP molecules adsorption on mild steel surface and forming a uniform inhibitive film. In the same way, the relaxation time constant ($\tau_{ct}$=$R_{ct}$× $C_{ct}$) values increase with inhibitor concentration as well and the time of adsorption process becomes therefore much higher which means a slow adsorption process [**35**]. This shows that there is an agreement between the amount of charge that can be stored (that is capacitance) and discharge velocity in the interface ($\tau_{ct}$) [**36**].

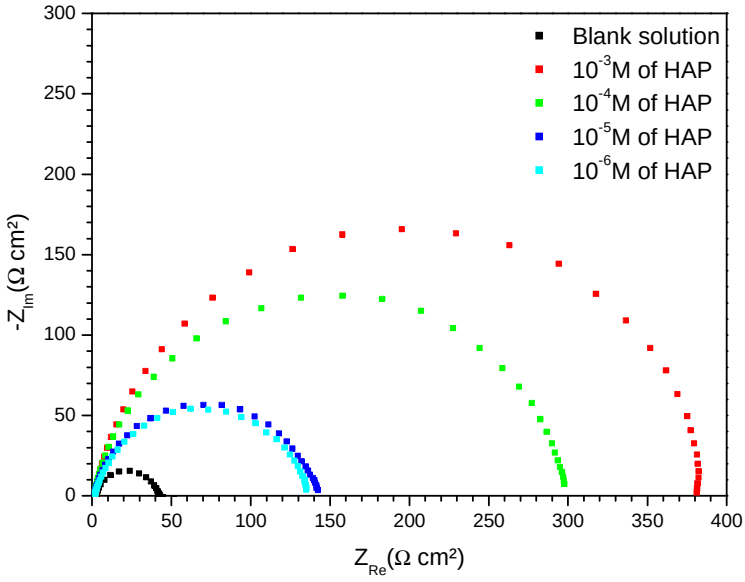


**Figure 3: Nyquist plots for mild steel in 1 M HCl containing different concentrations of HAP at open circuit potential**

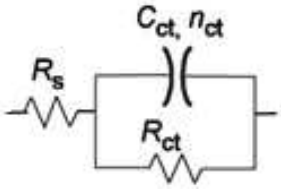


**Figure 4: Electrical equivalent circuits used for modeling the metal/solution interface**

**Table 3: Corrosion parameters for mild steel in 1 M HCl at various concentrations of HAP**

| Conc. (M) | $R_{ct}$ (Ω cm$^2$) | $C_{ct}$ (μF cm$^{-2}$) | $n_{ct}$ | $\tau_{ct}$(s) | $\eta_{EIS}$ (%) |
|---|---|---|---|---|---|
| 00 | 40 | 294 | 0.8 | 0.12 | 00 |
| $10^{-6}$ | 136 | 270 | 0.85 | 0.36 | 70.5 |
| $10^{-5}$ | 140 | 241 | 0.88 | 0.34 | 71 |
| $10^{-4}$ | 288 | 138 | 0.89 | 0.40 | 86 |
| $10^{-3}$ | 387 | 90 | 0.9 | 0.35 | 90 |

### 3.3. Effect of temperature

The effect of temperature on the inhibited acid–metal reaction is very complex, because many changes occur on the metallic surface such as rapid etching and desorption of inhibitor and the inhibitor itself may undergo decomposition. The potentiodynamic polarization curves of mild steel with and without $10^{-3}$ M of HAP at the temperature range from 298 to 328 K. The obtained results were presented in Figure 5. It is noted that the cathodic and anodic current–potential curves are giving rise to parallel lines. This shows that the increasing of temperature does not change the iron dissolution and hydrogen evolution mechanism. The oxidation of Fe and reduction of $H^+$ ions at the mild steel surface take place mainly through a charge transfer mechanism.

However, an inspection of Table 4 shown that, as the temperature increased, the values of $E_{corr}$ shift in the anodic direction, while the values of $i_{corr}$ increase and $\eta_{PP}$ decrease. This behavior reflects physical adsorption of HAP on the mild steel surface.

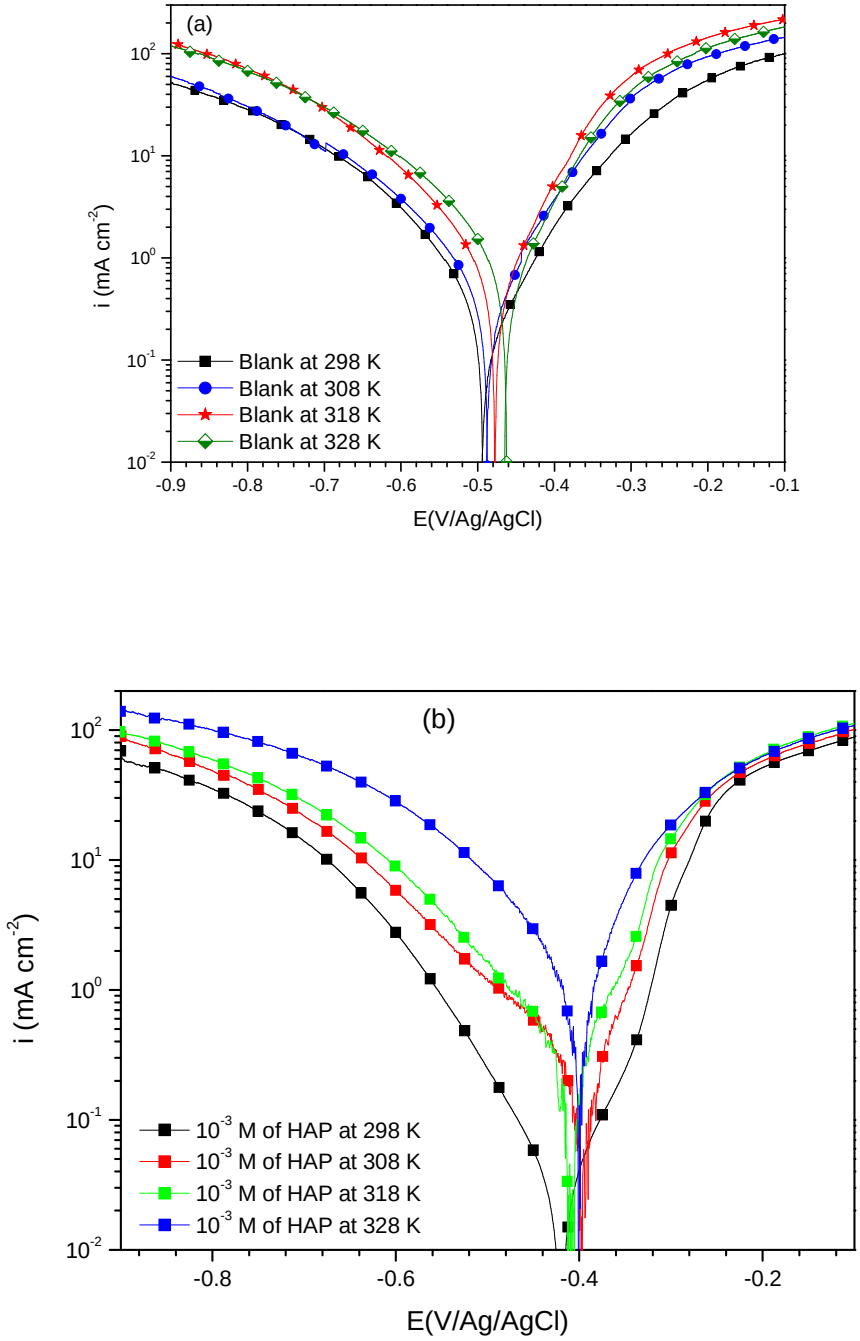


**Figure 5: Potentiodynamic polarization curves of mild steel in 1 M HCl at different temperatures (a) without and (b) with $10^{-3}$ M of HAP**

**Table 4: The influence of temperature on the electrochemical parameters for mild steel in 1M HCl and $10^{-3}$ M of HAP**

| | T (K) | $E_{corr}$ (mV/Ag/AgCl) | $i_{corr}$ (µA $cm^{-2}$) | $\eta_{PP}$ (%) |
|---|---|---|---|---|
| Blank solution | 298 | - 498 | 470 | - |
| | 308 | - 491 | 800 | - |
| | 318 | - 475 | 1470 | - |
| | 328 | - 465 | 2000 | - |
| $10^{-3}$ M of HAP | 298 | -419 | 43 | 91 |
| | 308 | -398 | 90 | 89 |
| | 318 | -411 | 162 | 89 |
| | 328 | -401 | 300 | 85 |

In addition, the $i_{corr}$ values were determined from the corresponding plots in order to calculate the activation energy of corrosion, which could give information about the mechanism of adsorption. The dependence of the corrosion rate on temperature can be expressed by the Arrhenius equation according to the following equation:

$$i_{corr} = A\exp\left(-\frac{E_a}{RT}\right) \quad (7)$$

Where $E_a$ is the apparent activation corrosion energy, T is the absolute temperature, A is the Arrhenius pre-exponential constant and R is the universal gas constant.

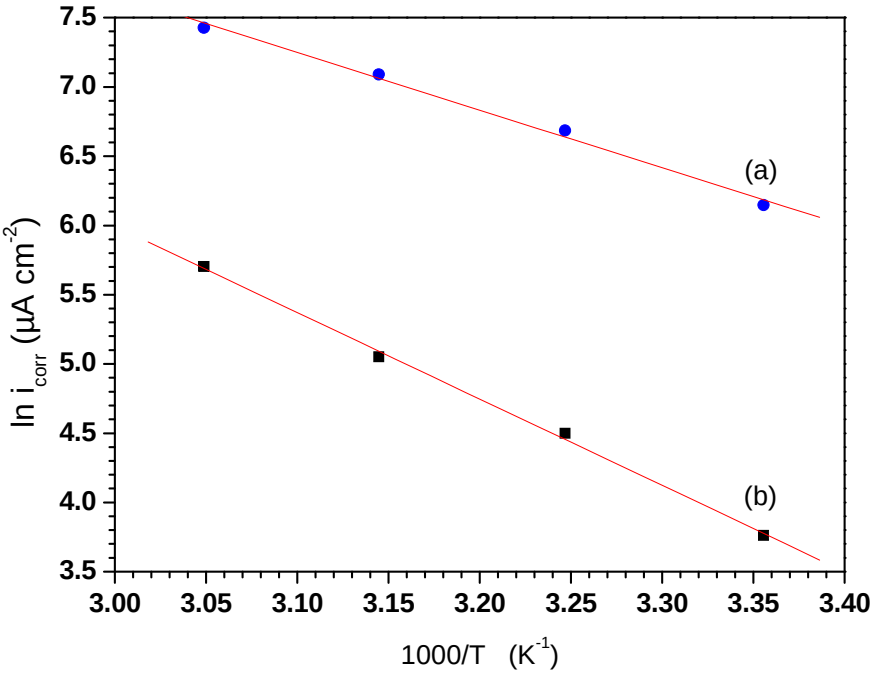


**Figure 6: Arrhenius plots for mild steel in 1 M HCl in (a) the absence and (b) presence of $10^{-3}$ M of HAP**

However, the $E_a$ values were calculated from Figure 6 as 34.6 KJ $mol^{-1}$ and 52 KJ $mol^{-1}$ in the absence and presence of HAP, respectively. The increase in activation energy in the presence of the inhibitor may suggest the physical adsorption [**37, 38**]. However, as it is also discussed in the literature [**39**] the adsorption process could not be classified as purely physical, which is the first stage of adsorption, or chemical. Moreover, the criteria of adsorption type obtained from the change of activation energy cannot be taken as a decisive due to competitive adsorption with water molecules, whose removal from the surface requires also some activation energy [**40**]. Therefore, it is concluded that, the adsorption of HAP molecules on the mild steel surface from 1 M HCl solution takes place through both physical and chemical processes simultaneously [**41**].

### 3.4. Effect of immersion time

The effect of immersion time was determined by expositing the mild steel with 1 M HCl solution in the absence and presence of HAP at the corrosion potential. The obtained results are given in Figure 7. It is noted that all plots contain a slightly depressed semi-circular shape and only one time constant was appeared indicating that the mild steel corrosion is mainly controlled by a charge transfer process. In this case, the similar equivalent electric circuit, Figure 4, with one time constants was proposed to reproduce these results by non linear regression calculation.

The most important data obtained from the equivalent circuit are presented in Table 5. It may be remarked that $R_{ct}$ value increases and $C_{ct}$ decreases with immersion time indicating that more inhibitor molecules are adsorbed on metallic surface and provided better surface coverage and/or enhanced the thickness of the protective layer at the metal/solution interface.

In addition, the change in the $C_{ct}$ values may be caused by the gradual replacement of water molecules by the adsorption of the inhibitor molecules on the metal surface, decreasing the extent of dissolution reaction. Thus the entire active sites become saturated with inhibitor. Moreover, $C_{ct}$ can be expressed as: $C_{ct} = \varepsilon \times \varepsilon_0 \times S/d$ (where ε is the relative dielectric constant, $\varepsilon_0$ is the dielectric constant in vacuum, S and d are the surface area and the thickness of the film, respectively) [**42**]. Thus, the decrease in the film capacitance values can be explained by the thickening of the film [**43**].

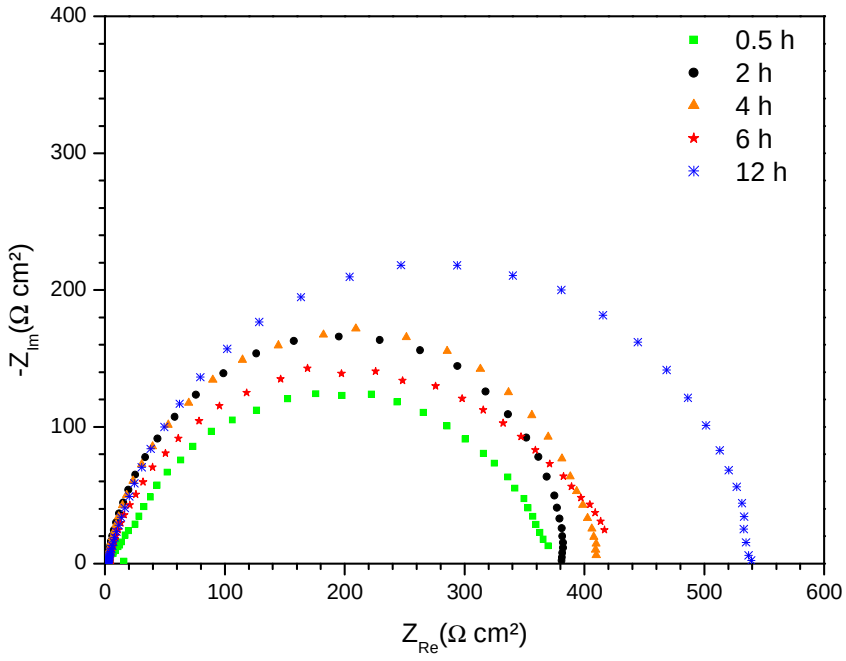


**Figure 7: Nyquist plots for mild steel in 1 M HCl containing 10-3 M of HAP at different immersion time (T=298 K)**

**Table 5: The influence of immersion time on the electrochemical parameters for mild steel in 1 M HCl in the presence of $10^{-3}$ M of HAP**

| Immersion time (h) | $R_{ct}$ (Ω cm$^2$) | $C_{ct}$ (μF cm$^{-2}$) | $n_{ct}$ | $\tau_{ct}$(s) | $\eta_{EIS}$ (%) |
|---|---|---|---|---|---|
| 0.5 | 387 | 90 | 0.9 | 0.35 | 90 |
| 2 | 390 | 92 | 0.89 | 0.36 | 90 |
| 4 | 418 | 81 | 0.88 | 0.34 | 90 |
| 6 | 428 | 75 | 0.87 | 0.32 | 91 |
| 12 | 541 | 70 | 0.9 | 0.38 | 92 |

### 3.4. Adsorption isotherm

The adsorption of inhibitor molecule on metal surfaces is a substitutional process, in which the adsorbed water molecules on metal surfaces are replaced by the inhibitor molecules. Several adsorption isotherms can be used to assess the adsorption behavior of such an inhibitor **[44].** Langmuir adsorption isotherm can be expressed by the following equation:

$$\frac{C_{inh}}{\theta} = \frac{1}{k_{ads}} + C_{inh} \qquad (8)$$

Plots of $C_{inh}/\theta$ as function of $C_{inh}$ yielded a straight line, as shown in Figure 8. The linear association coefficient ($R^2$) is almost equal to 1 ($R^2$ = 0.9999), and the slope is nearly 1, indicating that the adsorption of HAP molecules on the mild steel surface is described well by the Langmuir adsorption model.

Where $K_{ads}$ is the equilibrium constant for the adsorption/ desorption process and $C_{inh}$ is the inhibitor concentration in the electrolyte, which is related to the standard free energy of adsorption ( $\Delta G^*_{ads}$ ) according to Equation 9:

$$\Delta G^{*}_{ads} = -RT\,(\,Ln\,55{,}5\,K_{ads}\,) \qquad (9)$$

The negative value of $\Delta G^{*}_{ads}$ calculated from Equation (9), are consistent with the spontaneity of the adsorption process and the stability of the adsorbed layer on the carbon steel surface. Generally, values of $\Delta G^{*}_{ads}$ up to -20 kJ $mol^{-1}$ are consistent with physisorption, while those around -40 kJ $mol^{-1}$ or higher are associated with chemisorption as a result of the sharing or transfer of electrons from organic molecules to the metal surface to form a coordinate bond **[45]**. In the present work the value of $\Delta G^{*}_{ads}$ is equal to -43.1 KJ $mol^{-1}$. The large value of $\Delta G^{*}_{ads}$ and its negative sign is usually characteristic of strong interaction and a highly efficient adsorption **[46]**. Therefore, it is concluded that, the adsorption of HAP molecules on the mild steel surface is a mixed type of chemical and physical adsorptions with predominantly the first one [**47**–**49**].

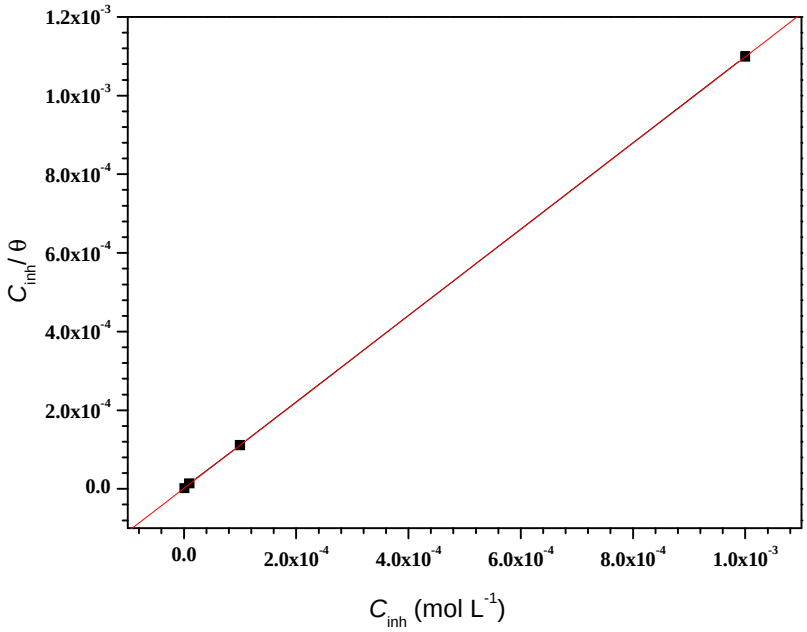


**Figure 8: Langmuir adsorption of HAP on the mild steel surface in 1 M HCl solution**

## CONCLUSION

The corrosion inhibition of mild steel in 1 M HCl solution by hydroxyapatite (HAP) was studied using electrochemical techniques. According to experimental findings, it could be concluded that:

1. HAP is a good corrosion inhibitor for the mild steel protection in 1 M HCl solution. The inhibitory efficiency of this compound depends on its concentration.
2. HAP acts by reducing the rates of both anodic and cathodic reactions. It is classified at a mixed type inhibitor.
3. The high inhibition efficiency of the inhibitor was explained by adsorption of the HAP molecules on the steel surface and a protective film formation.
4. HAP takes its performance at the temperature range 298 K- 328 K.
5. The adsorption of the inhibitor improved with immersion time by the increasing of the thickness film.
6. The adsorption of HAP on the steel surface from 1 M HCl solution follows Langmuir adsorption isotherm. The thermodynamic parameters suggest that this inhibitor is strongly adsorbed on the mild steel surface.

## REFERENCES

[1] K Mocachi, A. Hamel, R. Kherat, *Revue des énergies Renouvelables*, **2008**, 11(3), 357-362.
[2] AFGC. Cefracor, , Réhabilitation du biton armé dégradé par la corrosion, Centre Français Anticorrosion, **2003**.
[3] B. Grosgogeat, P. Colon, la corrosion, Université Médicale Virtuelle Francophone **2010**.

[4] D. Landolt, Corrosion et Chimie de Surfaces des Métaux, Vol.12, Presse Polytechniques et Universités Ramandes. **1993**
[5] F. Abdelali; Thèses de doctorat, Université Mentouri Constantine. **2007**.
[6] M.S. Morad, *J. Appl. Electrochem*., **2005**, 35, 889.
[7] H. Akrout, L. Bousselmi, E. Triki, S.Maximovitch, F. Dalard, *J. Mater. Sci*., **2004**, 39, 7341.
[8] M.S. Morad, A.A. Hermas, M.S. Abdel Aal, *J. Chem. Technol. Biotechnol*., **2002**, 77, 486.
[9] G. Kardas, R. Solmaz, *Corros. Rev.*, **2006**, 24, 151.
[10] G. Kardas, *Mater. Sci*., **2005**, 41, 337.
[11] R. Solmaz, G. Kardas, B. Yazıcı, M. Erbil, *Prot. Met.*, **2007**, 43, 476.
[12] E. Oguzie, Y. Li, F.H.Wang, *J. Colloid Interface Sci.*, **2007**, 310, 90.
[13] S. Sugiyama, J.B. Moffat, *Catal. Lett.*, **2001**, 76, 1.
[14] S. Sugiyama, E. Nitta, H. Hayashi, J.B. Moffa, *Catal. Lett.*, **1999**, 59, 67.
[15] S. Sugiyama, K. Abe, H. Hayashi, J.B. Moffat, *Catal. Lett.*, **1999**, 57, 161.
[16] S. Sugiyama, Y. Iguchi, T. Minami, H. Hayashi, *Catal. Lett*., **1997**, 46, 279.
[17] B. Liptakova, M. Hronec, Z. Cvengrosova, *Catal. Today*, **2000**, 61,143.
[18] I.D. Smiciklas, S.K. Milonji, C.S. Zec, *J. Mater. Sci*., **2000**, 3, 2825.
[19] R. Giovannini, R. Freitag, *Bioseparation*, **2001**, 9,359.
[20] X.G. Chen, J.V. Wright, J.L. Conca, L.M. Peurrung, *Water Air Soil Pollut*., **1997**, 98, 57.
[21] C.K. Danny, J.F. Porter, G. McKay, *Water Res*., **2001**, 35, 3876.
[22] I.S. Neira, Y.V. Kolenko, O.I. Lebedev, G. Van Tende- loo, H.S. Gupta, F. Guitian, M. Yoshimura, *Cryst. Growth Des*., **2009**, 9, 466.
[23] M. Stern, A.L. Geary. Electrochemical Polarization: A Theoretical Analysis of the Shape of Polarization Curves , *J. Electrochem. Soc*., **1957**, 104, 56-63
[24] A. Bouckamp, Users Manual Equivalent Circuit, Ver. 4.51, **1993**.
[25] C.M. Goulart, A. Esteves-Souza, C.A. Martinez-Huitle, C.J.F. Rodrigues, M.A.M. Maciel, A. Echevarria, *Corros. Sci.*, **2013**, 67, 281–291.
[26] A.Y. Musa, A.A.H. Kadhum, A.B. Mohamad, M.S. Takriff, *Corros. Sci.*, **2010**, 52, 3331–3340.
[27] L. Li, X. Zhang, J. Lei, J. He, S. Zhang, F. Pan, *Corros. Sci*., **2012**, 63, 82–90.
[28] I. Ahamad, M.A. Quraishi, *Corros. Sci.*, **2009**, 51, 2006–2013.
[29] M.A. Hegazy, A.M. Badawi, S.S. Abd El Rehim, W.M. Kamel, *Corros. Sci*., **2013**, 69, 110-122.
[30] A. Zarrouk, H. Zarrok, R. Salghi, B. Hammouti, F. Bentiss, R. Touir, M. Bouachrine, *J. Mater. Environ. Sci.*, **2013**, 4, 177–192.
[31] H. Gerengi, K. Darowicki, G. Bereket, P. Slepski, *Corros. Sci*., **2009**, 51, 2573.
[32] G.J. Brug, A.L.G. Van Den Eeden, M. Sluyters-Rehbach, J.H. Sluyters. *J. Electroanal. Chem*., **1984**, 176, 275-295.
[33] M. Moradi, J. Duan, X. Du, *Corros. Sci*., **2013**, 69, 338–345.
[34] Y. Tang, F. Zhang, S. Huc, Z. Cao, Z. Wu, W. Jing, *Corros. Sci*., **2013**, 74, 271–282.
[35] A. Popova, M. Christov, A. Vasilev, *Corros. Sci*., **2011**, 53, 1770–1777.
[36] K.F. Khaled, M.M. Al-Qahtani, *Mater. Chem. Phys*., **2009**, 113, 150–158.
[37] B. Xu, Y. Liu, X. Yin, W. Yang, Y. Chen, *Corros. Sci*., **2013**, 74, 206–213.
[38] A. Anejjar, A. Zarrouk, R. Salghi, H. Zarrok, D. Ben Hmamou, B. Hammouti, B. Elmahi, S.S. Al-Deyab, *J. Mater. Environ. Sci*., **2013**, 4, 583–592.
[39] Ramazan Solmaz, *Corros. Sci*., **2014**, 79, 169–176
[40] L. Vracar, D.M. Drazic, *Corros. Sci*., **2002**, 44, 1669–1680.
[41] Y. Tang, F. Zhang, S. Huc, Z. Cao, Z. Wu, W. Jing, *Corros. Sci*., **2013**, 74, 271–282.
[42] P. Gimenez, D. Petit, M. Badia, *Mater. Sci*., Forum 8, **1986**, 315.
[43] R. Touir, N. Dkhireche, M. Ebn Touhami, M. Sfaira, O. Senhaji, J.J. Robin, B. Boutevin, M. Cherkaoui, *Mater. Chem. Phys*., **2010**, 122, 1–9
[44] J.M. Bastidas, P. Pinilla, E. Cano, J.L. Polo, S. Miguel, *Corros. Sci*., **2003**, 45, 427– 449.].
[45] S.A. Refay, F. Taha, A.M. Abd El-Malak, *Appl. Surf. Sci*., **2004**, 236, 175.
[46] M. Abdallah, *Corros. Sci*., **2002**, 44, 717.
[47] X. Li, S. Deng, H. Fu, *Corros. Sci*., **2011**, 53, 302–309.
[48] S. Deng, X. Li, H. Fu, *Corros. Sci*., **2011**, 53, 822–828
[49] I. Ahamad, R. Prasad, M.A. Quraishi, *Corros. Sci*., **2010**, 52, 3033–3041.